Am J Physiol Regul Integr Comp Physiol 307: R1167–R1179, 2014.
First published August 6, 2014; doi:10.1152/ajpregu.00188.2014.

Guanylin peptides regulate electrolyte and fluid transport in the Gulf toadfish (*Opsanus beta*) posterior intestine

Ilan M. Ruhr,[1] Charlotte Bodinier,[1] Edward M. Mager,[1] Andrew J. Esbaugh,[1] Cameron Williams,[1] Yoshio Takei,[2] and Martin Grosell[1]

[1]*Rosenstiel School of Marine and Atmospheric Science, University of Miami, Miami, Florida; and* [2]*Ocean Research Institute, University of Tokyo, Tokyo, Japan*

Submitted 6 May 2014; accepted in final form 5 August 2014

Ruhr IM, Bodinier C, Mager EM, Esbaugh AJ, Williams C, Takei Y, Grosell M. Guanylin peptides regulate electrolyte and fluid transport in the Gulf toadfish (*Opsanus beta*) posterior intestine. *Am J Physiol Regul Integr Comp Physiol* 307: R1167–R1179, 2014. First published August 6, 2014; doi:10.1152/ajpregu.00188.2014.—The physiological effects of guanylin (GN) and uroguanylin (UGN) on fluid and electrolyte transport in the teleost fish intestine have yet to be thoroughly investigated. In the present study, the effects of GN, UGN, and renoguanylin (RGN; a GN and UGN homolog) on short-circuit current (I_{sc}) and the transport of Cl^-, Na^+, bicarbonate (HCO_3^-), and fluid in the Gulf toadfish (*Opsanus beta*) intestine were determined using Ussing chambers, pH-stat titration, and intestinal sac experiments. GN, UGN, and RGN reversed the I_{sc} of the posterior intestine (absorptive-to-secretory), but not of the anterior intestine. RGN decreased baseline HCO_3^- secretion, but increased Cl^- and fluid secretion in the posterior intestine. The secretory response of the posterior intestine coincides with the presence of basolateral NKCC1 and apical cystic fibrosis transmembrane conductance regulator (CFTR), the latter of which is lacking in the anterior intestine and is not permeable to HCO_3^- in the posterior intestine. However, the response to RGN by the posterior intestine is counterintuitive given the known role of the marine teleost intestine as a salt- and water-absorbing organ. These data demonstrate that marine teleosts possess a tissue-specific secretory response, apparently associated with seawater adaptation, the exact role of which remains to be determined.

guanylin; uroguanylin; HCO_3^-; CFTR; osmoregulation; fluid secretion

REGULATION OF SALT, WATER, and acid-base balance by the osmoregulatory organs of teleost fish is a vital process for maintaining homeostasis in a diverse range of habitats and is accomplished through various compensatory responses. To combat diffusive fluid loss, marine teleosts drink seawater (SW) and absorb both salts and water in the intestine (56). It is well established that the absorptive-type $Na^+/K^+/2Cl^-$-cotransporter NKCC2 (SLC12a1) transports salts down their electrochemical gradient from the intestinal lumen across the apical membrane into the enterocytes (18, 33, 62). More recently, an additional pathway for Cl^- absorption, by SLC26a6 (an apical Cl^-/HCO_3^- antiporter), was identified to exchange intestinal Cl^- for intracellular HCO_3^- and is responsible for up to 70% of Cl^- uptake (26, 29, 43, 63). Fluid absorption follows absorption of osmolytes via these two ion-uptake pathways. In addition, titration of HCO_3^- (to form CO_2 and H_2O) by protons (H^+) extruded by an apical v-type H^+-ATPase (VHA) and precipitation of HCO_3^- with intestinal Ca^{2+} and Mg^{2+} (to form Ca- and $MgCO_3$ precipitates) facilitates fluid absorption by lowering intestinal fluid osmolality (21, 23, 25, 29, 64–66). Ultimately, absorption of salts, coupled to base secretion, allows for solute-coupled and osmotic fluid absorption.

Although the marine teleost intestine is vital to salt and fluid absorption, it also exhibits secretory characteristics with respect to Cl^- and fluid. Studies have identified possible pathways for both Cl^- secretion, via an apical cystic fibrosis transmembrane conductance regulator (CFTR) channel, and fluid secretion into the intestinal lumen by marine teleosts (48, 58, 68), both of which are common in terrestrial animals (16, 32). It has been proposed that the function of apical CFTR is to facilitate Cl^- and fluid secretion for the elimination of toxins from the intestine (48, 55). However, neither the exact function nor the regulatory pathways responsible for switching intestinal ion and fluid absorption to secretion are known.

Guanylin (GN) and uroguanylin (UGN) are upstream regulators of apical CFTR and modulate intestinal Na^+, Cl^-, fluid, and HCO_3^- fluxes in mammals (3, 50, 61). GN and UGN bind to guanylyl cyclase-C (GC-C), a transmembrane receptor on the apical membrane of intestinal tissues (50, 52, 53), causing an intracellular transduction cascade that increases the formation of cyclic guanosine monophosphate (cGMP). cGMP can either stimulate cGMP-dependent protein kinase (PKG) or lead to increases in cyclic adenosine monophosphate (cAMP) levels that stimulate cAMP-dependent protein kinase (PKA); both PKG and PKA activate CFTR (3, 4, 9, 13, 34, 42). In mammals, this leads to Cl^-, fluid, and HCO_3^- secretion into the intestinal lumen to help neutralize the effects of acidic chyme (2, 5, 30, 54). This process is especially important after the ingestion of food, where GN and UGN are secreted into the intestine, bind GC-C, and elevate the levels of intracellular cGMP in enterocytes (3).

GN, UGN, and renoguanylin (RGN) are also present in teleost fish; intestinal tissues express GN and UGN, while renal tissue express UGN and RGN (10, 12, 39, 67). Although the physiological function of the guanylin peptides in teleosts is still uncertain, studies have shown that they may play a role in long-term salinity adaptation. Indeed, GN and UGN mRNA expression increase following a 24-h transfer from freshwater (FW) to SW by at least twofold in the Japanese eel (*Anguilla japonica)* (12, 39, 67), a pattern also observed in the rat after salt loading of intestinal tissues (8, 40, 45). In mammalian tissues, GN and UGN either increase the secretory short-circuit current (I_{sc}) of the intestine or reverse an absorptive I_{sc}, while in teleosts, these peptides have no effect on the anterior intestine of the Japanese eel, but do reverse the I_{sc} of the mid and posterior intestine, resulting in a net serosa-to-mucosa flux of, presumably, Cl^- ions (38, 54, 68).

Address for reprint requests and other correspondence: I. M. Ruhr, Rosenstiel School of Marine and Atmospheric Science, Univ. of Miami, Miami, FL (e-mail: iruhr@rsmas.miami.edu).

Table 1. *Sequences of primers for cDNA cloning*

Name	Sequence
GUA-S1 (GN-F)*	5′-ATCTGCGCTAATGCTGCCTGCAC-3′
RevGUA-S1 (GN-R)*	5′-GTGCAGGCAGCATTAGCGCAGAT-3′
tfGN-F	5′-AGCAAAGGGCAGCATCTGCA-3′
tfGN-R	5′-TGGCAAGATGTTTGTGGCTTTGC-3′
tfUGN-F†	5′-CCGACCCTCTCATGCCGCAGG-3′
tgUGN-R†	5′-TGCACGGAGGCATCGAGCTG-3′
Universal primer‡	5′-CTAATACGACTCACTATAGGGCAAG CGTGGTATCAACGCAGAGT-3′ 5′-CTAATACGACTCACTATAGGGC-3′

*Designed sense primers taken and/or modified from Yuge et al. (67). †Gene-specific primers designed from annotated Gulf toadfish transcriptome. ‡Universal primer (Clontech SMARTer RACE cDNA Amplification Kit) consists of both a long and short sequence.

However, considering that the intestine of marine teleosts must absorb water to avoid dehydration and that the guanylin peptides cause fluid secretion in mammalian intestinal cells, would marine teleosts respond to these peptides in a similar manner? Evidence from the Japanese eel supports the view of net fluid secretion into the intestinal lumen, due to the reversal of the I_{sc} in the mid and posterior intestine by GN, UGN, and RGN (68). These observations would suggest that marine teleosts secrete fluid into the intestinal lumen via the guanylin peptide-induced activation of the intracellular cascade that occurs in mammals. However, it remains to be confirmed that the secretory current is conducted by Cl^- and whether this current promotes fluid secretion. Moreover, the molecular components of the secretory ion transport pathway have yet to be firmly established.

The purpose of this study was to further characterize the physiological effects of the guanylin peptides in marine teleost fish by investigating their effects on Gulf toadfish (*Opsanus beta*) intestinal epithelium. A secretory short-circuit current response to luminal application of the guanylin peptides was anticipated and hypothesized to *1*) be most pronounced in the posterior intestine, *2*) be driven by net secretion of Cl^-, and *3*) be associated with net fluid secretion and enhanced HCO_3^- secretion. Furthermore, it was hypothesized that *4*) a secretory pathway would be present in the guanylin-responsive segments of the intestine.

MATERIALS AND METHODS

Experimental animals. Gulf toadfish (*Opsanus beta*) were caught as bycatch from a local shrimp fisherman in Biscayne Bay, FL. Immediately upon arrival in the laboratory, the Gulf toadfish were briefly placed in a FW bath (3 min) and then treated with malachite green to remove ectoparasites, following the protocol from McDonald et al. (49). Gulf toadfish were separated by size, and 8–10 fish were placed in 62-liter tanks, with a continuous flow-through of sand-filtered SW from Biscayne Bay (30–34 ppt salinity, 26–29°C). Gulf toadfish were fed to satiation weekly, but food was withheld for 72 h before experimentation. Fish husbandry and experimental procedures were performed according to an approved University of Miami Animal Care Protocol (Institutional Animal Care and Use Committee No. 10–293, renewal 02). All Gulf toadfish used for experimentation were killed using 0.2 g/l MS-222 (Argent) solution buffered with 0.3 g/l $NaHCO_3^-$, followed by severing of the spinal cord at the cervical vertebra.

cDNA cloning. Cloning was performed using cDNA constructed from homogenized Gulf toadfish intestinal tissues (60). Partial cDNAs of a GN-like and a UGN-like peptide were cloned by 3′- and 5′-rapid amplification of cDNA ends (RACE) using a universal primer and designed-sense primers (Table 1). PCR amplifications were performed according to a modified protocol from Yuge et al. (67) using Taq DNA polymerase and buffer (Invitrogen). After 3′- and 5′-RACE procedures were performed, gene-specific primers (Table 1) were used in PCR reactions to determine the full sequence of the GN and UGN prohormones.

Composition of salines, hormones, and inhibitors. Japanese eel GN, UGN, and RGN peptides were resuspended into 10^{-3} mol/l stock solutions in nano-pure water. The final concentrations for the guanylin peptides in the luminal saline were 10^{-9}-10^{-5} mol/l. Luminal (pH 7.0) and serosal (pH 7.8) salines were prepared as per Table 2. When using the pH-stat titration system, luminal pH was maintained at 7.8 by titration using a 0.005 N HCl solution. Bafilomycin (Enzo Life Sciences) was used to inhibit the apical VHA and prepared in DMSO at 1.0 mmol/l for application in a final concentration of 2 μmol/l and 0.1% DMSO, which has been previously used in the Gulf toadfish (27, 31). CFTRinh-172 (Sigma) was used to inhibit a putative apical CFTR channel (1, 6, 7, 48) and prepared in DMSO at 1.0 mmol/l for application in a final concentration of 10 μmol/l and 0.1% DMSO, which is in the mid-range solubility limit for this blocker (1).

In vitro short-circuit current, transepithelial potential, and HCO_3^- secretion experiments on isolated intestinal tissue: effects of Japanese eel guanylin peptides. To measure the effects of Japanese eel guanylin peptides (GN, UGN, and RGN) on I_{sc}, transepithelial potential (TEP), and transepithelial conductance (G_{te}), Ussing chambers (Physiological Instruments) were employed. Segments of anterior and posterior intestine from each experimental Gulf toadfish (ranging from 20 to 30 g) were excised, cut open, and mounted onto tissue holders (model P2413; Physiological Instruments), which exposed 0.71 cm^2 of excised tissue, and were positioned between two half-chambers (model 2400; Physiological Instruments). Each half-chamber contained 2 ml of appropriately gassed mucosal or serosal saline (Table 2). Salines in each half-chamber were continually mixed by airlift gassing with either 100% O_2 (mucosal) or 0.3% CO_2 in O_2 (serosal) (Table 2), as described in Genz and Grosell (19). The temperatures of the salines in the chambers were maintained at 25°C. Current and voltage electrodes were connected to amplifiers (model VCC600; Physiological Instruments) and, depending on the experiment, recorded either differences in I_{sc} under voltage-clamp conditions at 0.0 mV, with 3 s of 1-mV pulses (mucosal-to-serosal) at 60-s intervals, or differences in TEP under current-clamp conditions at 0.0 μA, with 3 s of 10-μA pulses (mucosal-to-serosal), also at 60-s intervals. Epithelial conductance

Table 2. *Composition of salines for short-circuit current and pH-stat titration experiments*

Compound	Mucosal*	Serosal
NaCl, mmol/l	69.0	151.0
KCl, mmol/l	5.0	3.0
$MgSO_4$, mmol/l	77.5	0.88
$MgCl_2$, mmol/l	22.5	
Na_2HPO_4, mmol/l		0.5
KH_2PO_4, mmol/l		0.5
$CaCl_2$, mmol/l	5.0	1.0
HEPES, free acid, mmol/l		3.0
HEPES salt, mmol/l		0.003
Urea, mmol/l		4.5
Glucose, mmol/l		5.0
Osmolality, mosmol/kgH_2O†	310	310
pH	7.8‡	7.8
Gas§	100% O_2	0.3% CO_2 in O_2

*Mucosal application of guanylin, uroguanylin, or renoguanylin (10^{-9}–10^{-5} mol/l). †Adjusted with mannitol to ensure transepithelial isosmotic conditions in all experiments. ‡pH 7.80 was maintained by pH-stat titration. §Salines were gassed for at least 1 h before experimentation.

(G_{te}) was determined from inflections in I_{sc} and TEP during pulsing using Ohms law. I_{sc} and TEP measurements were recorded on a computer using BIOPAC systems Acqknowledge software (v. 3.8.1).

To simultaneously measure electrophysiological parameters (TEP) and HCO_3^- secretion on the isolated intestinal tissues, Ussing chambers were set up in tandem with a pH-stat titration system (TIM 854 or 856 Titration Managers; Radiometer), as outlined previously (24). A pH electrode (model PHC4000.8; Radiometer) and a microburette tip (from which acid was delivered) was submersed in the luminal half-chamber to allow for pH readings and pH-stat titrations. Mucosal salines (injected into the luminal half-chamber) were maintained at a physiological pH of 7.8, throughout all experiments, to allow for symmetrical pH conditions on either side of the epithelium. The pH values and rate of acid titrant (0.005 mol/l HCl) additions were recorded onto personal computers using the Titramaster software (v. 5.1.0). Epithelial HCO_3^- secretion rates were calculated from the rate of titrant addition and its concentration, as described in Grosell and Genz (24).

To determine the dose response and effective concentrations of the three eel peptides, GN, UGN, and RGN were added to the luminal half-chamber in a dose-dependent manner (10^{-9}-10^{-5} mol/l), as described in Takei and Yuge (59), while I_{sc} was recorded. Luminal peptide concentrations were increased once stable I_{sc} readings were reached. The length of time to reach a stable reading varied according to individual preparations, resulting in a range of time courses for the peptide and intestinal segment studied (GN: AI 189–452 min, PI 180–369 min; UGN: AI 243–399 min, PI 155–440 min; and RGN: AI 176–372 min, PI 254–449 min). All subsequent experiments were performed using only RGN due to limited supplies of GN and UGN.

To determine if the secretory anion flux observed following peptide addition was due to the activation of apical CFTR, the CFTR inhibitor CFTRinh-172 was added to the luminal half-chamber before the addition of RGN, while TEP and HCO_3^- secretion were recorded. To determine if observed, and unexpected, reductions in HCO_3^- secretion following peptide addition were due to stimulation of apical H^+ secretion, the VHA inhibitor, bafilomycin, was added to the luminal half-chamber simultaneously with RGN. Because the effects of bafilomycin can be transient (27, 31), bafilomycin and RGN were added concurrently, rather than in sequence, to capture the immediate effects of this inhibitor on the tissues.

Vehicle controls using 0.1% DMSO ($n = 5$) showed no impact of DMSO on the tissue response to RGN for either I_{sc} or HCO_3^- secretion (data not shown).

Dependence of HCO_3^- secretion on mucosal Cl^- concentration. Considering the unexpected reduction in HCO_3^- secretion following peptide addition, the dependence of HCO_3^- secretion on mucosal Cl^- concentrations was examined. Low Cl^- levels were achieved by replacing Cl^- salts with corresponding gluconate salts, while higher levels were achieved by partially replacing $MgSO_4$ with $MgCl_2$. The pH-stat titration experiments were limited in time (~1 h per flux period) as serosal-to-mucosal Cl^- flux, as well as Cl^- leaking from the pH electrode, contributed to altered Cl^- concentrations during the flux period, especially during low-Cl^- conditions. HNO_3, rather than HCl, was used as titrant in these experiments in an attempt to reduce Cl^- contamination. All experiments were initiated with a control flux (standard mucosal saline, Table 2, Cl^- concentration = 129 mmol/l), and then a subsequent flux with Cl^--manipulated saline. Subsamples of the mucosal saline during the second flux were obtained at the beginning and end of each flux to verify actual luminal Cl^- concentrations. Secretion rates of HCO_3^- from the second flux period are expressed as a fraction of the initial control secretion rates.

Intestinal sac preparations. Intestinal sac preparations were used to examine the net flux of water, HCO_3^-, Cl^-, and Na^+ across the anterior and posterior intestinal epithelia, and followed a modified protocol from Genz and Grosell (19). The entire length of the intestine was excised from an adult Gulf toadfish and cut distally to the pyloric sphincter and proximally to the rectal sphincter. A PE50 catheter was inserted into the anterior end of the excised intestine and tied off with a silk suture. The appropriate mucosal saline (Table 2) was then injected into the catheter to rinse the intestine of any debris, precipitates, and intestinal fluids. The anterior portion of the intestine was then tied off with a silk suture and cut to make the anterior sac preparation. The mid intestine was discarded, while a new PE50 catheter was inserted into the posterior portion and the distal end was tied off to make the posterior sac. Two mucosal salines were used for this experiment (Table 2): control mucosal saline and treatment mucosal saline containing 5×10^{-8} mol/l RGN. The volume of injected mucosal saline was determined by weighing a 5-ml syringe before and after filling (Table 2). After an intestinal preparation was filled with appropriate mucosal saline, the intestinal sac was blot-dried and weighed; it was then placed in a scintillation vial filled with 15 ml of serosal saline gassed with 0.3% CO_2. The preparations were left for a 2-h flux period, after which each intestinal sac was blot-dried and weighed, and its mucosal saline was collected. The sac tissue itself was then cut down its midline, spread onto tracing paper, and traced to measure its surface area. Subsamples of mucosal saline were collected at the beginning and end of the 2-h flux period.

Water, HCO_3^-, Cl^-, and Na^+ from the mucosal samples were analyzed using the following methods. HCO_3^- equivalents were calculated by the Henderson-Hasselbalch equation, using mucosal pH values, total CO_2 (measured by a Corning 965 carbon dioxide analyzer) readings from individual intestinal sac preparations, and a pK of 9.46 (29). Concentrations of Na^+ were measured using flame spectrometry (Varian 220FS), while Cl^- concentrations were measured using anion chromatography (DIONEX 120). The fluxes for these ions were calculated from the differences between the initial and final amounts of each ion, taking into account the flux period and tissue surface area. Water flux was calculated by taking the difference between the initial and final volume (mass) of each intestinal sac, also taking into account the flux period and tissue surface area.

Immunohistochemistry. The anterior and posterior intestinal segments were excised from adult Gulf toadfish, from which CFTR, NKCC (for both NKCC1 and -2), and NKA were immunolocalized following a modified protocol from Bodinier et al. (6, 7). After dissection, intestinal tissues were fixed in Z-fix (Anatech) for 48 h, followed by a 1-wk immersion in 70% ethanol. Tissues were then dehydrated in ascending grades of ethanol (3 washes in 95%, followed by 3 washes in 100%). Following dehydration, tissues were prepared for wax imbedding by immersing them in two washes of butanol, followed by two washes with Histochoice (Amresco). Tissues were finally immersed in four washes of paraplast (McCormick Scientific) and imbedded. Serial sections (4 μm) were cut from the tissues using a Leitz microtome (model 1512). Sections were transferred and mounted onto poly-L-lysin-coated slides and dried for 24 h at 37°C. Slides were then prepared for antibody treatment by immersing them into two washes of Histochoice (Amresco), five washes of decreasing alcohol (100→50% ethanol), and one wash in PBS. Subsequently, slides were incubated in 10 mmol/l citric acid solution and placed in a microwave for two 5-min incubations to reveal antigenic sites. Slides were then immersed in 0.01% Tween-20 in PBS, followed by immersion in a 5% skim milk solution, and three washes in PBS. Primary antibody (10 μg/ml) was dissolved in 0.5% skim milk in PBS, added to each slide, and incubated for 1 h at 37°C. The primary antibodies consisted of monoclonal mouse CFTR (R&D Systems), polyclonal goat NKCC1, and polyclonal rabbit NKA (Santa Cruz Biotechnology). After the 1-h incubation, slides were immersed in three PBS washes. The secondary antibodies consisted of anti-mouse IgG, anti-goat IgG, and anti-rabbit IgG (Alexa Fluor 488, 350, and 568, respectively, from Invitrogen). Slides were once again incubated in 37°C for 1 h, followed by three successive washes in PBS. Coverslips were placed on the slides using ProLong Gold Antifade Reagent (Molecular Probes). Control slides were treated with the same conditions, but without primary antibody. Slides were observed with an Olympus fluorescent microscope (u-tvo.5xc-2), with attached

QImaging camera (Retiga EXi, Fast 1394); iVision and Fiji software were used to analyze images.

Statistical analyses. Data are presented as absolute means ± SE. Means were compared for significant differences using Student's or paired *t*-tests, Mann-Whitney rank sum tests, and one-way repeated-measures ANOVA tests as appropriate. The Holm-Sidak test was used, when appropriate, for all multisample comparison tests. All *t*-tests are two-tailed unless stated otherwise. SigmaStat 3.5 and SigmaPlot 11.0 were used for statistical analyses and to calculate EC_{50} values. Means were considered significantly different when $P < 0.05$.

RESULTS

cDNA cloning. Two distinct guanylin-like peptides and their prepropeptides were cloned from Gulf toadfish intestinal cDNA, revealing peptides of 108 and 109 amino acids (Fig. 1). The two cloned peptide variants differ at amino acid residues 1, 3, 9–11, and 13 (Fig. 1). They were sufficiently different from one another to identify them as Gulf toadfish GN (tfGN) and Gulf toadfish UGN (tfUGN), after comparing them to the sequences of birds, mammals, reptiles, and teleosts (Fig. 2). In addition, these putative tfGN and tfUGN peptides were verified by comparing their nucleotide sequences (Fig. 1) to identical sequences found in the intestinal transcriptome of the Gulf toadfish.

Moreover, tfGN differed from Japanese eel GN and RGN at residues 1, 3, and 8, and at residues 1 and 3, respectively. tfUGN exhibited greater variation than GN and differed from Japanese eel UGN and RGN at residues 1, 3, 10, 11, and 13, and at residues 1, 9–11, and 13, respectively (Fig. 2).

Effects of eel guanylin peptides on I_{sc}. The effects of eel GN, UGN, and RGN on dissected Gulf toadfish tissues mounted in Ussing chambers are clear. A one-way, repeated-measures ANOVA revealed that the I_{sc} of the anterior intestine ($n = 6$ for all treatments) remained unchanged (Fig. 3, *A–C*), while in the posterior intestine, there was a significant reversal of the I_{sc} (from mucosa-to-serosa to serosa-to-mucosa), due to the eel guanylin peptides, in a dose-dependent manner (Table 3). The maximal ΔI_{sc} in the posterior intestine due to eel GN, UGN, and RGN ($n = 5$, 6, and 6, respectively) occurred at concentrations of $\geq 10^{-7}$, 10^{-7}, and 2×10^{-7} mol/l (Fig. 3, *D–F*), respectively, with EC_{50} values of 5.82×10^{-8} (GN), 4.90×10^{-8} (UGN), and 1.16×10^{-8} (RGN) mol/l. The differences observed in response to the eel peptides in the posterior intestine are in agreement with those from a previous report (68). Differences in G_{te} values between the anterior and posterior intestinal segments, independent of the dose of the three eel guanylin peptides, were significant (Table 4). No differences in G_{te} across doses in the anterior intestine were observed, but G_{te} increased in the posterior intestine in a dose-dependent manner for all three eel guanylin peptides, matching the changes in observed I_{sc} (Table 4).

Effects of eel RGN on HCO_3^- secretion. Surprisingly, mucosal application of eel RGN to the posterior intestinal tissue, mounted in an Ussing chamber-pH-stat titration system, significantly reduced HCO_3^- secretion, depressing the mean secretion rate between 13.3 and 21.2% (Fig. 4*A*). Additionally, the TEP of the posterior tissues significantly decreased 30 min after exposure to RGN (Fig. 4*B*). However, G_{te} remained unaffected after mucosal application of RGN, with a mean value of 5.6 ± 0.1 mS/cm^2.

To examine if the observed inhibition of HCO_3^- secretion in the posterior intestine due to RGN may have been caused by a downstream effect of RGN acting on the apical VHA, both bafilomycin and RGN were applied to the mucosal saline in an Ussing chamber-pH-stat titration system. Following the results of the previous experiment, a one-way, repeated-measures ANOVA revealed that this treatment reduced the mean HCO_3^- secretion rate by 12.9–34.5% after mucosal application (Fig. 5*A*). The TEP also decreased significantly 30 min after treatment with RGN and bafilomycin (Fig. 5*B*). Similarly to the previous experiment, G_{te} remained unaffected after treatment (4.68 ± 0.12 mS/cm^2). Mean HCO_3^- secretion rates in Figs. 4*A* and 5*A*, in the pre-RGN-treated (control) tissues, fall within the range previously reported for the Gulf toadfish posterior intestine (21, 31).

Intestinal sac preparations: Na^+, Cl^-, water, and HCO_3^- fluxes. As hypothesized, a one-tailed test revealed that eel RGN resulted in a significant stimulation of a secretory Cl^- flux in the posterior intestine (Fig. 6*B*), while no effect was present in either the control tissues or in the eel RGN-treated anterior intestinal tissues. However, in both the anterior and posterior intestinal sac preparations, there were no differences in Na^+

Guanylin

```
 M  K  A  T  F  T  A  I  V  L  L  V  F  A  L  A  S  A  S  E  A  V  Q  V  H  E
ATGAAGGCCACGTTCACCGCCATTGTGCTCCTCGTCTTTGCTCTCGCTTCGGCTTCAGAGGCGGTGCAAGTCCACGAG    78
 G  G  L  S  F  S  L  E  A  V  K  K  L  Q  E  L  T  E  S  G  D  A  V  Q  A  Q
GGCGGATTGTCATTCTCACTGGAAGCCGTGAAGAAGCTCCAGGAGCTGACAGAGAGCGGCGATGCGGTGCAAGCACAA   156
 S  P  R  L  L  V  R  N  N  A  V  C  D  N  P  E  L  P  E  E  L  L  P  L  C  K
AGTCCTCGCCTCCTGGTGCGCAACAACGCCGTCTGTGACAACCCCGAACTCCCAGAGGAGCTCCTGCCCCTCTGCAAG   234
 Q  R  A  A  S  A  S  F  A  R  L  A  M  V  P  M  D  V  C  E  I  C  A  F  A  A
CAAAGGGCAGCATCTGCATCGTTCGCCAGACTAGCGATGGTTCCCATGGACGTGTGTGAGATCTGCGCTTTTGCTGCC   312
 C  T  G  C
TGCACTGGATGC                                                                      324
```

Uroguanylin

```
 M  K  L  L  T  V  A  V  A  L  T  L  C  L  C  S  V  A  A  D  V  H  V  K  V  G
ATGAAGCTGCTGACTGTTGCCGTGGCTCTGACCTTGTGTTTGTGCAGCGTGGCTGCAGACGTGCACGTGAAGGTTGGA    78
 E  K  S  F  P  L  E  A  V  K  R  L  K  E  L  T  D  L  D  G  H  V  S  P  H  L
GAAAAGAGCTTCCCCTTGGAGGCAGTCAAGCGGCTGAAGGAGCTGACGGATCTGGACGGCCACGTCAGCCCTCATCTC   156
 T  A  A  N  V  A  A  V  C  A  D  P  L  M  P  Q  V  F  Q  A  A  C  Q  E  N  A
ACCGCGGCGAATGTTGCAGCTGTTTGTGCCGACCCTCTCATGCCGCAGGTCTTTCAGGCGGCGTGCCAAGAGAACGCA   234
 A  A  I  V  F  S  K  L  V  Y  I  I  T  P  L  D  L  C  E  I  C  A  N  P  S  C
GCAGCCATTGTTTTCTCCAAATTAGTGTATATTATCACGCCTTTGGATCTCTGTGAAATTTGTGCCAATCCCTCCTGC   312
 Y  G  C  L  N
TATGGATGTCTGAAC
```

Fig. 1. cDNA sequences of guanylin and uroguanylin prohormones from the intestine of the Gulf toadfish. 3′- and 5′-rapid amplification of cDNA ends (RACE) reactions were performed to acquire overlapping portions of each transcript using degenerate primers, based on the nucleotide sequences of mature peptides (boxed) from several teleost species. Subsequently, full prohormone sequences were obtained using gene-specific primers, resulting in peptides of 108 (guanylin) and 109 (uroguanylin) amino acids in length.

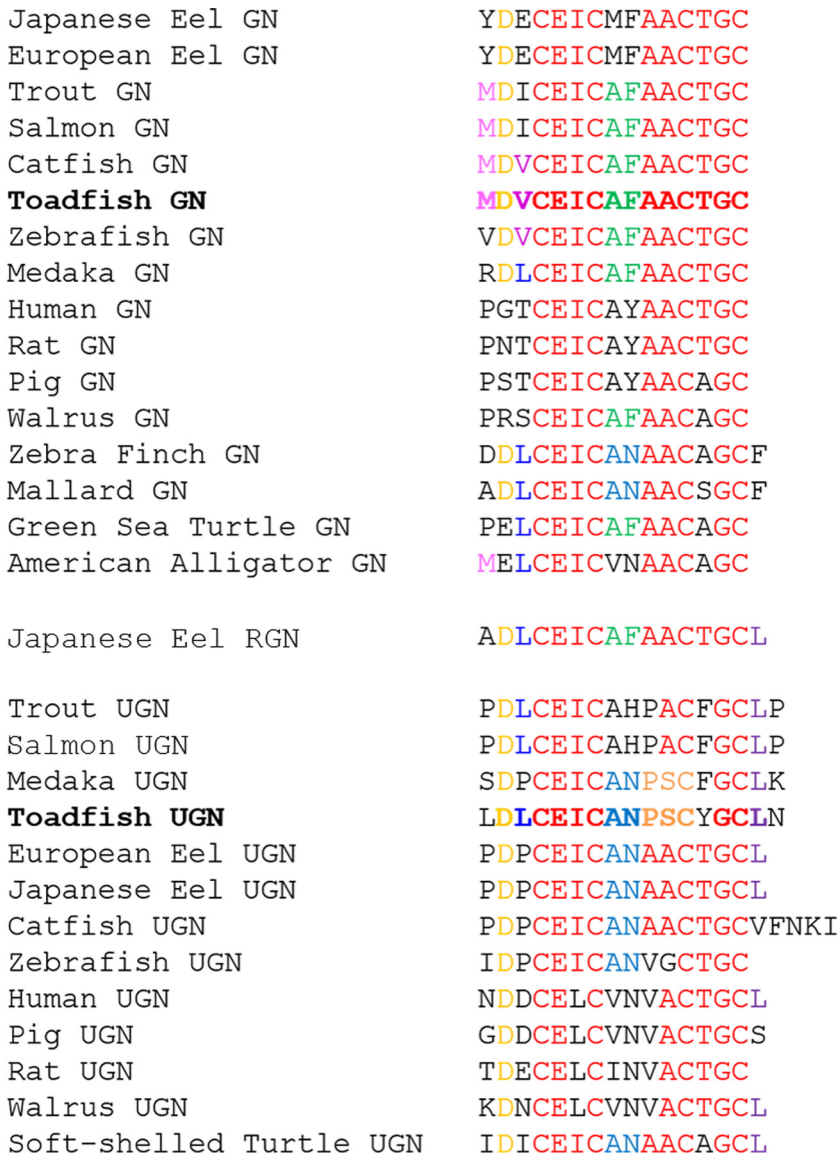

Fig. 2. Sequence comparisons of mature guanylin (GN), uroguanylin (UGN), and renoguanylin (RGN) from various bird, mammalian, reptilian, and teleost species. Gulf toadfish amino acid residues from GN and UGN that are identical to those of other species are color coded and in bold. Amino acid residues in red are conserved across most species and illustrate the close sequence homology of the guanylin peptides. Other conserved regions are described as follows. The amino acid, D, at the second position in yellow corresponds to the same sequence in both GN and UGN of the Gulf toadfish. Amino acids in pink (1st position; M), light purple (3rd position; V), and green (8th and 9th position; AF) correspond only to Gulf toadfish GN, while amino acids in dark blue (3rd position; L), light blue (8th and 9th position; AN), orange (10th-12th position; PSC), and dark purple (16th position; L) correspond only to Gulf toadfish UGN. NCBI ascension numbers are in order from *top* to *bottom*. GN: AB080640.1, FM173262.1, BX866654, CA045042, CK402502, KJ549666, CD759824, BJ877267, M95174, M93005, Z73607, XM_004406665.1, XM_002189797.2, XM_005014992.1, EMP42088.1, and XM_006278378.1; RGN: AB080641.1; UGN: BX3093850, CA041361, BJ512940, KJ549667, FM173261.1, AB080642.1, CK401577, CD283474, U34279, Z83746, U14322, and XP_004406740.1.

flux between control and eel RGN-treated tissues (Fig. 6*A*). As for water, a one-tailed test revealed that eel RGN stimulation resulted in significant net fluid secretion in the posterior intestinal sacs (Fig. 6*D*), while no effects were present in control tissues or eel RGN-stimulated anterior intestinal sacs. Contradictory to our hypothesis, however, a one-tailed test revealed that eel RGN significantly decreased HCO_3^- secretion (similarly to the pH-stat titration experiment) by roughly 34% in the posterior intestinal sacs (Fig. 6*C*) compared with controls or eel RGN-treated anterior intestinal sacs.

Effects of CFTRinh-172 and RGN on ion transport across the posterior intestine. Neither treatment with CFTRinh-172 nor with subsequent treatment of RGN in the mucosal half-chamber of an Ussing chamber affected the HCO_3^- secretion rate in the posterior intestine (Fig. 7*A*). CFTRinh-172 did not affect posterior intestinal TEP; however, as with previous experiments, RGN did cause a significant decrease in TEP despite being applied after CFTRinh-172 (Fig. 7*B*). The typical stimulation of I_{sc} by RGN was prevented by pretreatment with CFTRinh-172 (Fig. 7*C*). Similarly to the previous experiments, G_{te} remained unaffected across all treatments with a mean value of 6.08 ± 1.00 mS/cm^2. It is worth mentioning that 5-nitro-2-(3-phenylpropylamino) benzoic acid (NPPB), a known CFTR blocker used in the Japanese eel (68), was initially tested. However, application of NPPB alone resulted in a net secretory I_{sc}, similarly to that produced by the eel peptides (possibly acting as a general Cl^- transporter blocker). Thus, CFTRinh-172 was used in the present study.

Dependence of HCO_3^- secretion on mucosal Cl^- concentration. Contrary to expectations, intestinal HCO_3^- secretion rates were unaffected by luminal Cl^- concentrations (Fig. 8) within the range tested (3.8–154.8 mmol/l).

Immunohistochemistry: tissue-specific differences in histology. Differences between the anterior and posterior intestine (n = 3) concerning the presence of apical CFTR, apical NKCC2, basolateral NKA, and basolateral NKCC1 were observed. In the anterior intestine, NKCC1-like, NKCC2-like, and NKA-like immunoreactivity was observed in the enterocytes (Fig. 9*A*). These same transporters were also observed in the posterior intestine, along with CFTR-like immunoreactivity

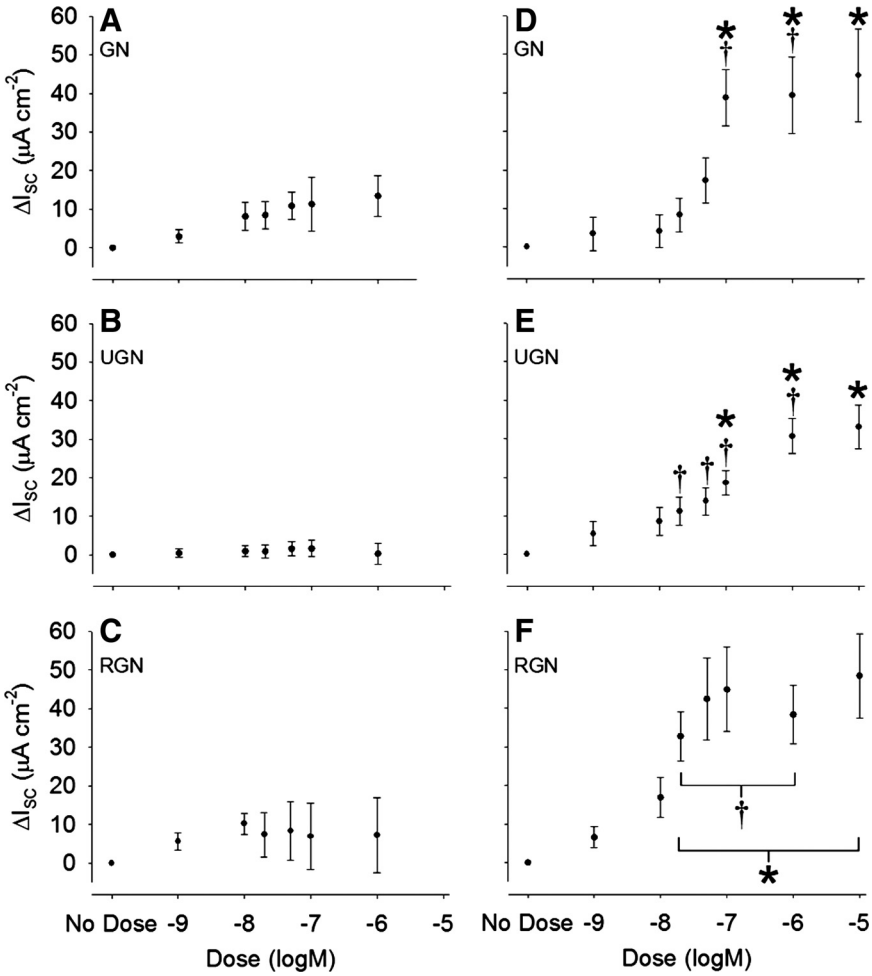

Fig. 3. Dose-dependent effects of mucosal application of GN (*A* and *D*), UGN (*B* and *E*), and RGN (*C* and *F*) on the short-circuit current (I_{sc}) of anterior and posterior intestinal epithelia. Values are represented as the difference in short-circuit current (ΔI_{sc}) from control (no dose) conditions as a function of peptide concentration. Anterior intestinal (*A–C*) tissues were dosed with 10^{-9}-10^{-6} mol/l (M) of the peptides, while posterior intestinal (*D–F*) tissues were dosed with 10^{-9}-10^{-5} mol/l of the peptides. Values are means ± SE (n = 5–6). *Significant effects of increasing dose within a tissue; †significant differences ($P < 0.05$) between anterior and posterior intestine.

in the apical membrane (Fig. 9, *B* and *C*). These results indicate distinct differences in apical CFTR localization between the anterior and posterior intestine and are in agreement with previous reports of other marine teleost species (6, 46, 48).

DISCUSSION

Tissue-specific responses to eel GN, UGN, and RGN. Despite the evolutionary distances between the selected animal classes listed in Fig. 2, the amino acid sequences of GN and UGN are remarkably well conserved. In the majority of sequences across species and animal classes, the amino acid residues 4–8 (CEICA), 10–12 (AAC), and 14–15 (GC) do not differ. Eel RGN produced effects in the intestine of both the Gulf toadfish and Japanese eel, presumably because of its high degree of similarity to GN from both these species. Thus, despite these minor differences, our initial analyses gave us confidence that the Japanese guanylin peptides could be used to stimulate physiological responses in the Gulf toadfish tissue.

Table 3. *Short-circuit current of the anterior and posterior intestine in response to guanylin, uroguanylin, and renoguanylin*

	I_{sc}, μA/cm^2							
Dose, mol/l	Control	10^{-9}	10^{-8}	2×10^{-8}	5×10^{-8}	10^{-7}	10^{-6}	10^{-5}
GN								
AI	−25.4 ± 16.6	−7.5 ± 2.6	−5.5 ± 2.9	−20.3 ± 17.9	−18.3 ± 18.4	−25.5 ± 23.2	−28.0 ± 26.2	
PI	−22.3 ± 15.4	−18.8 ± 18.8	−18.1 ± 18.2	−14.0 ± 17.9	−5.0 ± 18.67	14.5 ± 24.9*	17.0 ± 20.0*	22.2 ± 20.8*
UGN								
AI	−8.8 ± 6.8	−8.4 ± 7.3	−7.9 ± 8.0	−8.0 ± 8.1	−7.3 ± 8.4	−4.0 ± 8.8	−5.4 ± 9.4	
PI	−25.9 ± 4.6	−21.0 ± 4.0	−17.7 ± 3.9	−7.0 ± 8.7	−5.0 ± 8.1	−1.5 ± 6.7*	9.5 ± 5.3*	12.5 ± 6.4*
RGN								
AI	−7.3 ± 2.5	−1.7 ± 3.7	1.4 ± 3.0	−4.5 ± 5.9	−6.1 ± 5.2	−8.6 ± 5.4	−9.3 ± 5.5	
PI	−30.2 ± 3.07	−23.6 ± 3.9	−13.3 ± 5.8	2.6 ± 8.4*	12.3 ± 12.5*	14.7 ± 12.8*	6.2 ± 8.0*	18.3 ± 12.9*

Values are means ± SE; n = 5–6 for the responses of each anterior and posterior intestinal segment to guanylin (GN), uroguanylin (UGN), and renoguanylin (RGN), respectively. I_{sc}, short-circuit current; AI, anterior instestine; PI, posterior intestine. Peptides were applied to the mucosal half-chamber (2-ml volume) of an Ussing chamber in a cumulative manner. Negative mean values denote net absorption, while positive mean values denote net secretion. The time course for each experiment varied among individuals (see text for details). *Significant effects of increasing dose within a tissue from the control.

Table 4. *Transepithelial conductance of the anterior and posterior intestine in response to guanylin, uroguanylin, and renoguanylin*

	G_{te}, mS/cm^2							
Doses, mol/l	Control	10^{-9}	10^{-8}	2×10^{-8}	5×10^{-8}	10^{-7}	10^{-6}	10^{-5}
GN								
AI†	8.86 ± 1.06	8.69 ± 1.22	8.41 ± 2.42	8.41 ± 1.68	8.97 ± 1.50	8.46 ± 2.69	9.38 ± 1.89	
PI	6.62 ± 1.44	7.00 ± 1.25	6.97 ± 1.22	7.37 ± 1.04	7.22 ± 1.16	7.16 ± 1.22	7.34 ± 1.37	8 ± 1.12*
UGN								
AI†	11.03 ± 0.36	11.33 ± 0.54	11.30 ± 0.57	10.98 ± 0.35	11.37 ± 0.43	11.51 ± 0.53	11.59 ± 0.52	
PI	6.29 ± 0.50	6.10 ± 0.50	6.20 ± 0.54	6.22 ± 0.55	6.28 ± 0.63	6.17 ± 0.59	6.41 ± 0.55	7.32 ± 0.64*
RGN								
AI†	10.44 ± 0.33	10.29 ± 0.31	10.56 ± 0.28	10.63 ± 0.36	11.08 ± 0.26	11.27 ± 0.22	11.43 ± 0.39	
PI	5.94 ± 0.53	5.89 ± 0.53	5.89 ± 0.55	6.42 ± 0.74	6.65 ± 0.92	6.96 ± 0.88	6.63 ± 1.09	7.09 ± 1.04*

Values are means ± SE; $n = 5$–6 for the responses of each anterior and posterior intestinal segment to GN, UGN, and RGN, respectively. Peptides were applied to the mucosal half-chamber (2-ml volume) of an Ussing chamber in a cumulative manner. *Differences from the control within a tissue; †transepithelial conductance (G_{te}) value of the anterior intestine at any given dose is significantly greater than its counterpart value in the posterior intestine ($P < 0.05$).

Indeed, all eel guanylin peptides elicited robust responses from the Gulf toadfish posterior intestine, similarly to those observed in the Japanese eel and, in some cases, to mammalian intestinal epithelia as well. Moreover, the similarities in the amino acid sequences between eel RGN and tfGN may also explain the greater than fourfold difference in the EC_{50} value of eel RGN compared with eel GN and UGN.

The present study reveals that only the posterior portion of the Gulf toadfish intestine responds to mucosal application of eel GN, UGN, and RGN by reversing I_{sc}, causing net Cl^- and fluid secretion, and inhibiting HCO_3^- secretion. Changes in I_{sc}, due to guanylin peptide stimulation, have also been observed in the Japanese eel (68) and may be common to marine teleosts. The Gulf toadfish and Japanese eel responses are in contrast to the effects of GN and UGN in mammals, where both peptides act on the entire mammalian intestinal tract (5, 13, 15, 30, 42). A parsimonious explanation for the region-specific responses in the Gulf toadfish intestine to the guanylin peptides may be the distribution of possibly distinct GC-C receptor subtypes and their different affinities for the guanylin peptides. Indeed, GC-C1 and GC-C2 are two GC-C subtypes so far characterized in the European (*Anguilla anguilla)* and Japanese eels (11, 39, 69). Two subtypes, OlGC6 and OlGC9, are also expressed in medaka (*Oryzias latipes*) (36), while only one GC-C type has been found in mammals and it is the predominant GC in the

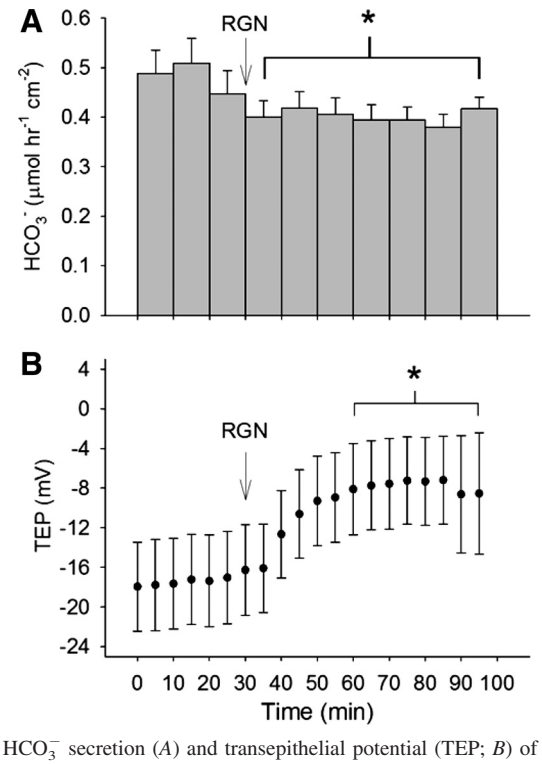

Fig. 4. HCO_3^- secretion (*A*) and transepithelial potential (TEP; *B*) of isolated posterior intestinal tissue following mucosal application of RGN (5×10^{-8} mol/l; indicated by the arrow) in Ussing chambers. Values are means ± SE ($n = 6$–7). *Significant differences ($P < 0.05$) in HCO_3^- secretion and in TEP from the control period (0–30 min).

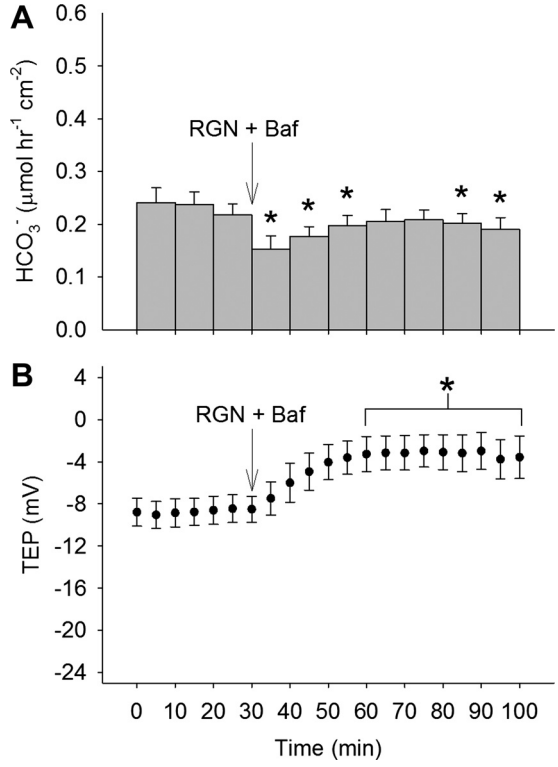

Fig. 5. HCO_3^- secretion (*A*) and TEP (*B*) of isolated posterior intestinal tissue exposed to mucosal doses of bafilomycin (Baf; 2 μmol/l) and RGN (5×10^{-8} mol/l), indicated by an arrow. Values are means ± SE ($n = 5$–6). *Significant differences ($P < 0.05$) from the control period (0–30 min).

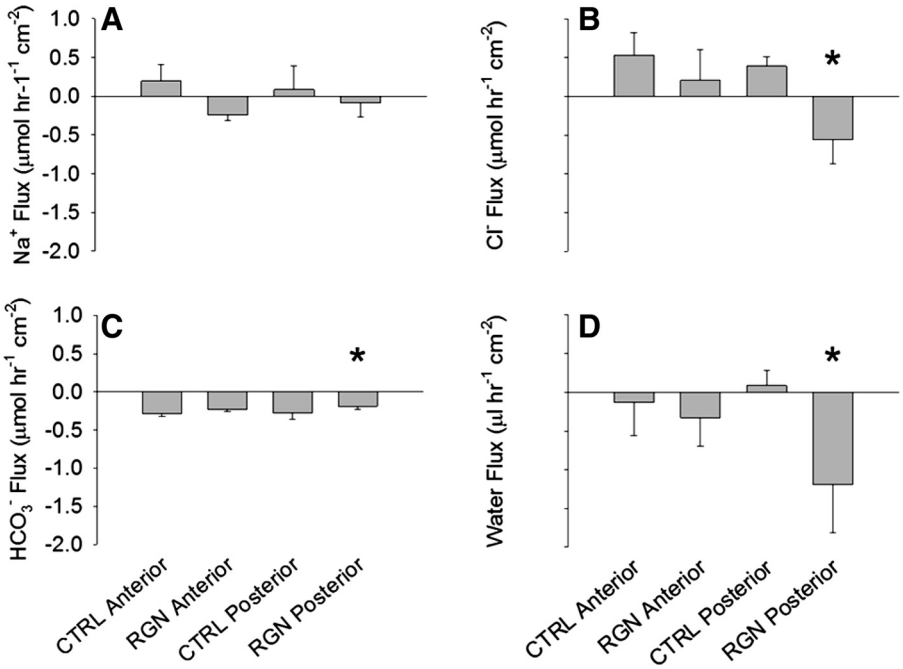

Fig. 6. Na^+ (*A*), Cl^- (*B*), water (*C*), and HCO_3^- (*D*) fluxes obtained from Gulf toadfish anterior and posterior intestinal sac preparations with and without luminal addition of RGN (5×10^{-8}). Negative and positive values indicate secretion and absorption, respectively. Values are means ± SE (n = 5–15). *Significant differences ($P < 0.05$) within a tissue [i.e., the control (CTRL) and treatment (RGN) groups].

intestine (4). Nonetheless, stimulation of fish and mammalian GC-Cs expressed in cell culture lines by GN or UGN leads to significant guanylyl cyclase activity and increases in cGMP (10, 13, 15, 36, 53, 69), yet, in the anterior intestine of marine teleosts, these increases may not be occurring in significant amounts (if at all) to produce the downstream effects observed in the posterior intestine.

An equally parsimonious alternative/additional explanation to describe the regional response of the Gulf toadfish intestine to the guanylin peptides may be the observation of both basolateral NKCC1-like and apical CFTR-like immunoreactivity in the posterior intestine. Expression of basolateral NKCC1 and apical CFTR is not uncommon in the posterior intestine of marine and SW-adapted euryhaline teleost species (6, 14, 35, 46, 48), which could form a secretory pathway for Cl^-.

Eel UGN elicited a weaker response from the Gulf toadfish posterior intestine than did eel GN and RGN (despite a lower EC_{50} value than eel GN), and this difference appears to be more pronounced than that observed in the Japanese eel (68). In the Japanese eel, GC-C1 binds preferentially to UGN, while GC-C2 is the predominant GN receptor (69). Although it is unknown if Gulf toadfish possess multiple GC-Cs, it is possible that the presence of multiple Gulf toadfish GC-Cs bind eel GN and UGN differentially, and it is conceivable that the posterior intestine of the Gulf toadfish expresses more of a GC-C subtype that binds favorably to eel GN and RGN over eel UGN. In addition, it cannot be ruled out that the experimental conditions applied in the present study affected peptide-receptor interactions. In rat intestinal tissues and in T84 cells expressing rat GC-C, for example, tissues were most sensitive to UGN in salines of pH 5.5, with GN being more effective between pH 7.4 and 8.0 (34, 38). It is plausible that UGN elicited a weaker I_{sc} reversal at the posterior intestine due to the pH of the mucosal saline used in this study (pH 7.8), which would interfere with its binding ability. However, the low pH hypothesis may not apply to teleost guanylin peptides as Yuge et al. (69) performed their experiments by applying eel guanylin peptides to a mucosal saline of pH 7.2, resulting in increases in intracellular cGMP levels in the Japanese eel.

Eel GN, UGN, and RGN reverse electrolyte and fluid transport in the posterior intestine. In the present study, the eel guanylin peptides reversed the I_{sc} of the Gulf toadfish posterior intestine from net absorptive to net secretory (Table 3). This secretory response is in accordance to those observed in the Japanese eel mid and posterior intestine (68), throughout the rat intestine (38), and in T84 cells (34). Conversely, the I_{sc} of the Gulf toadfish anterior intestine, as with the Japanese eel (68), was unaffected by either of the eel guanylin peptides (Fig. 3, *A–C*). The reversal of the posterior intestinal I_{sc} by eel RGN coincides with a reversal of Cl^- flux, which results in net Cl^- and fluid secretion into the intestinal sac preparations (Fig. 6*B*). This response is similar to that observed in mammalian tissues and in T84 cells, in which mucosal application of GN has been shown to significantly alter the I_{sc}, activate apical CFTR, and cause Cl^- and fluid secretion [for review in Forte (17)], and agrees with a GN-induced reversal of the I_{sc} of the Japanese eel mid and posterior intestine (68). Furthermore, in all Ussing chamber experiments performed in this study, mucosal application of eel RGN significantly decreased the serosa negative TEP of the posterior intestine, consistent with anion secretion (Figs. 4*B*, 5*B*, and 7*B*). Moreover, eel RGN increased G_{te} modestly, but significantly, in the I_{sc} studies on the posterior intestine; however, such increases were not observed in the subsequent studies and may be due to the dose of RGN to which we exposed tissues. In the I_{sc} experiments, only posterior intestinal tissues exposed to 10^{-5} mol/l GN, UGN, or RGN demonstrated significant increases in G_{te}. Curiously, while it appears that 5×10^{-8} mol/l RGN was sufficient to inhibit HCO_3^- secretion and reverse I_{sc}, it was insufficient to cause changes in G_{te}.

To determine if apical CFTR mediates the reversal of the I_{sc} at the posterior intestine, via net Cl^- secretion, we used

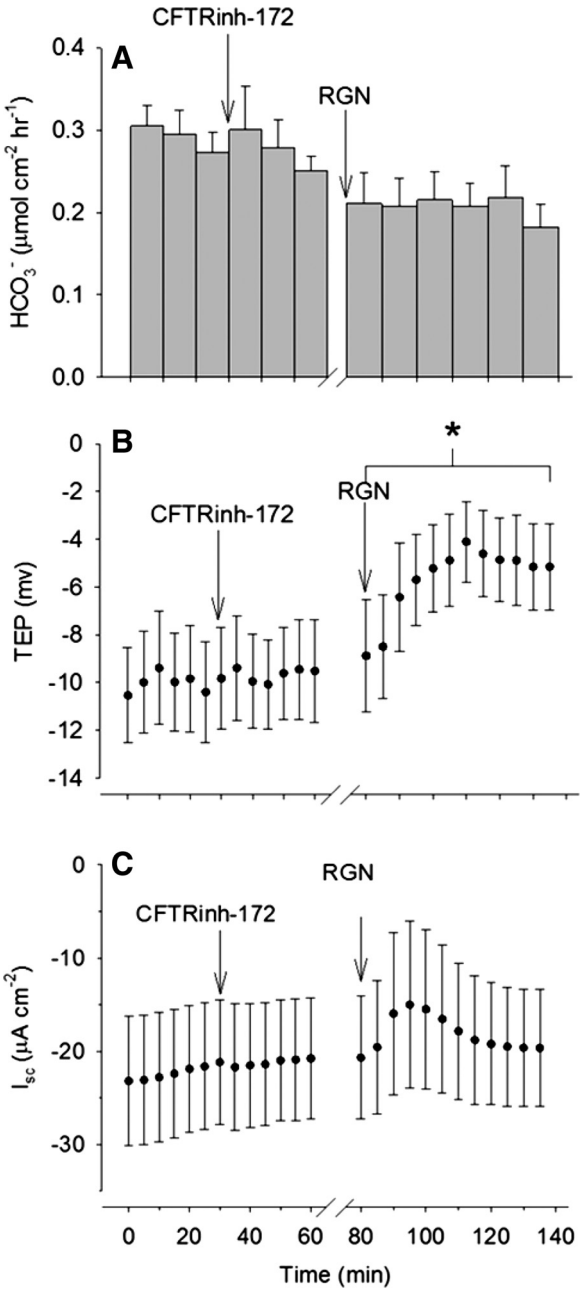

Fig. 7. HCO_3^- secretion (*A*), TEP (*B*), and I_{sc} (*C*) of isolated posterior intestinal tissue exposed to mucosal application of cystic fibrosis transmembrane conductance regulator (CFTR) inhibitor (CFTRinh-172; 10 μmol/l) and RGN (5×10^{-8} mol/l), indicated by arrows. Values are means ± SE (n = 5–6). *Significant differences ($P < 0.05$) from the control period (0–30 min).

CFTRinh-172, a known mammalian CFTR blocker (41). Yuge and Takei (68) demonstrated that simultaneously exposing Japanese eel intestinal tissues to NPPB, another CFTR inhibitor, and GN did not affect the absorptive I_{sc}, suggesting that Cl^- is secreted by apical CFTR. In the present study, exposing the Gulf toadfish posterior intestine to CFTRinh-172 prevented the RGN-stimulated change in I_{sc}. These results suggest that, as in mammals and in the Japanese eel, apical CFTR plays a primary role in Cl^- secretion by the intestine and is activated by the downstream effects of GC-C stimulation. Consistent with these observations is evidence of apical CFTR-like immunoreactivity in the posterior intestine, but not in the anterior intestine, of the Gulf toadfish.

Apical expression of CFTR in the intestine of marine and SW-adapted teleosts has been documented previously (6, 20, 48), and it has been revealed that apical CFTR expression may be important in SW adaptation (7). Moreover, the intestine of SW-adapted teleosts also expresses basolateral NKCC1 and apical NKCC2 (14, 20, 35). Immunohistochemisty in the present study also reveals apical expression of CFTR-like and NKCC2-like immunoreactivity, consistent with a previous report on the Gulf toadfish (62), and basolateral NKCC1-like immunoreactivity in the Gulf toadfish intestine. However, the distribution of these transporters is not uniform and the discontinuity of transporter types coincides with the present report's physiological findings of Cl^- secretion. In the anterior intestine, there is clear NKCC1-like and NKCC2-like immunoreactivity in the basolateral and apical membranes, respectively (Fig. 9*A*). Conversely, while NKCC1-like and NKCC2-like immunoreactivity is also found in the posterior intestine, apical CFTR-like immunoreactivity is present within this tissue as well (Fig. 9, *B* and *C*). These regional differences in transporter immunoreactivity correlate well with the region-specific differences in Cl^- and fluid secretion observed in this study. Although under normal conditions, NKCC2 acts as an important pathway for net Cl^- absorption by the marine teleost intestine, the effects of eel RGN in this study and those of GN and UGN in a previous report (68) lead to a reversal of the I_{sc} and result in net Cl^- secretion. Staining for NKCC1 and apical CFTR in the Gulf toadfish posterior intestine and the aforementioned eel RGN-induced Cl^- secretion suggest that NKCC1 and apical CFTR are stimulated, while NKCC2 may be inhibited, as suggested in the Japanese eel (68), to provide a conduit for Cl^- to travel from the blood, via the enterocytes, into the intestinal lumen (Fig. 10). Although the intracellular processes that lead to the activation of NKCC1 and apical CFTR, and possible inhibition of NKCC2, are unclear in fish, it is apparent that the guanylin peptides modify intracellular mechanisms to facilitate Cl^- and fluid secretion.

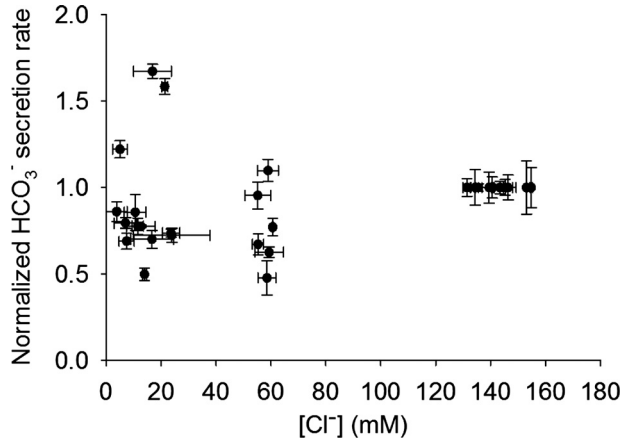

Fig. 8. HCO_3^- secretion rates by anterior intestinal epithelia as a function of mucosal Cl^- concentrations of the Gulf toadfish. Values are means ± SE. An initial control flux was measured using salines described in Table 1, before replacing luminal salines with different Cl^- levels. Data are presented as normalized to the HCO_3^- secretion rates during the initial 1-h control period. Horizontal error lines indicate the change in Cl^- concentration over time during the second flux period while vertical error bars indicate variation in HCO_3^- secretion rate over time during the second flux period.

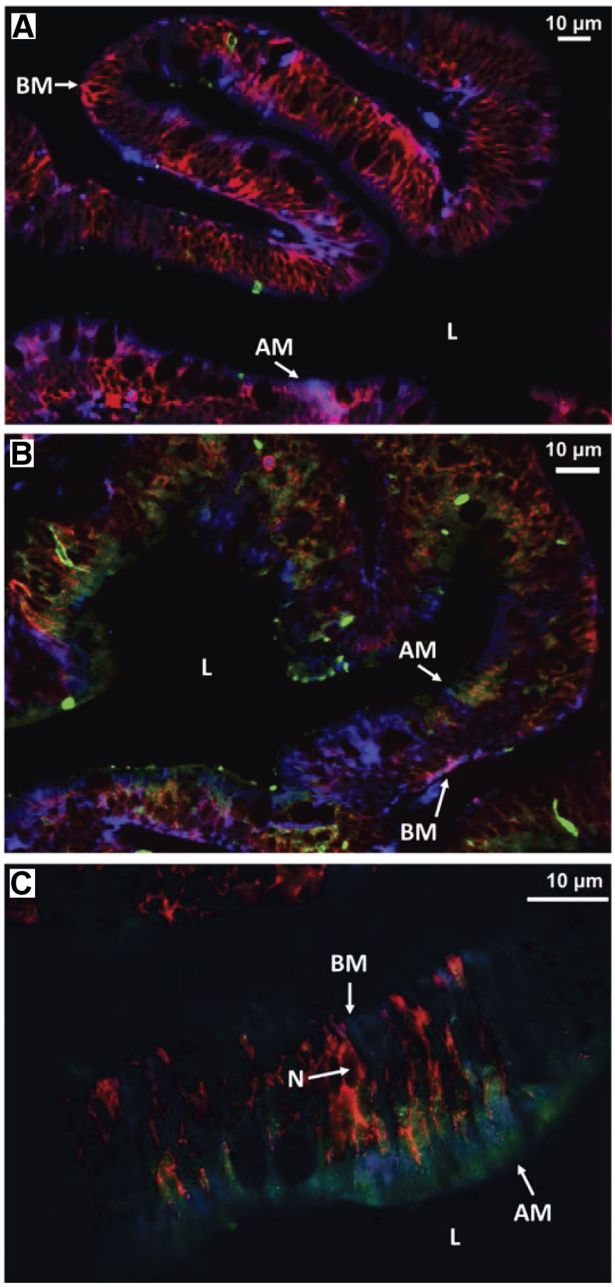

Fig. 9. Overlaid fluorescence image (×40 magnification) of NKA-like (red, basolateral), CFTR-like (green, apical), NKCC1-like (blue, basolateral), and NKCC2-like (blue apical) immunoreactivity in adult Gulf toadfish anterior (*A*) and posterior intestine (*B*). *C*: higher magnification image (×100) of the posterior intestine (showing presumed fluorescence for the three above-mentioned ion transporters), in which individual nuclei (N) can be clearly distinguished. AM, apical membrane; BM, basolateral membrane; L, lumen.

The present study also revealed an unexpected inhibition of HCO_3^- secretion, as opposed to the stimulatory effect observed in mammals. It has been shown that in mammalian intestinal tissues, using Cl^--free saline inhibits HCO_3^- secretion even in the presence of cAMP agonists (57), suggesting apical anion exchange. Terrestrial mammals are generally Cl^- limited, thus, an apical Cl^--secreting CFTR channel would fuel apical Cl^-/HCO_3^- by recycling Cl^- across the apical membrane (57), which does not seem to be the case for the Gulf toadfish. Accordingly, in mammals, HCO_3^- can be secreted into the intestine either through apical CFTR directly or by an apical anion exchanger that is secondary to Cl^- secretion via CFTR. To examine if a similar increase in HCO_3^- secretion in the Gulf toadfish was masked by an increase in VHA activity, bafilomycin was applied to inhibit this ATPase and revealed no effect of peptides on apical VHA (Fig. 5*A*). Consequently, in response to the guanylin peptides, it seems that mammals and marine teleosts modify HCO_3^- secretion oppositely from one another, yet, similarly, increase both Cl^- and fluid secretion.

The failure of the three eel guanylin peptides to increase HCO_3^- secretion in the Gulf toadfish intestine is perhaps in part explained by the lack of Cl^- limitation of the apical anion exchanger as demonstrated by the unaltered HCO_3^- secretion rates, even at luminal Cl^- concentrations in the low millimoles per liter range. It appears that the SLC26a6 anion exchanger, responsible for intestinal HCO_3^- secretion in the gulf toadfish (27), displays high Cl^- affinity. Furthermore, our observations provide evidence that Gulf toadfish apical CFTR does not transport HCO_3^- [as has been suggested in mammalian and fish tissues (37, 59)], since mucosal application of CFTRinh-172 alone had no effect on the HCO_3^- secretion rate of the posterior intestine (Fig. 7*A*) and since stimulation of Cl^- secretion results in an inhibition, rather than stimulation, of HCO_3^-

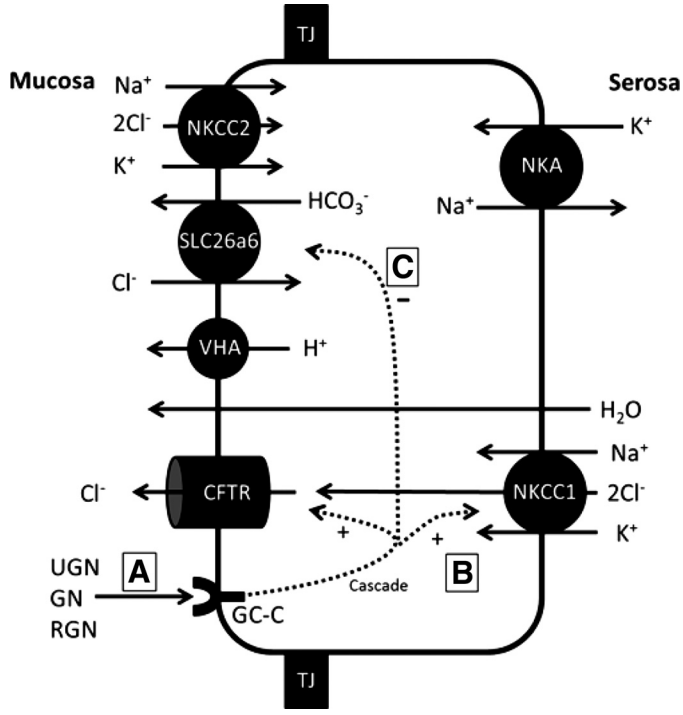

Fig. 10. Proposed effects of guanylin peptides in the posterior intestinal epithelia of Gulf toadfish (*Opsanus beta*). *A*: GN, UGN, or RGN bind to an apical guanylin cyclase-C receptor (GC-C), which initiates an intracellular transduction cascade. *B*: downstream effect of GC-C activation is the opening of a putative apical CFTR Cl^- channel and presumably activation of NKCC1, allowing Cl^- to cross the intestinal epithelia and enter the intestinal lumen. Water secretion is coupled to the induced secretory Cl^- flux. *C*: yet-to-be investigated mechanism either decreases the activity of the apical SLC26a6 anion exchanger or inhibits the transport of intracellular HCO_3^-. This decrease in HCO_3^- secretion is not a result of increased v-type H^+-ATPase (VHA) activity/H^+ excretion. +, Direct or indirect stimulatory effects; −, indicates direct or indirect inhibitory effects. TJ, tight junctions (Refs. 14, 22, 23, 44, 48).

secretion. The mechanisms for the eel RGN-induced inhibition of HCO_3^- secretion in the Gulf toadfish intestine are unknown and require further investigation.

Could inhibition of HCO_3^- enhance fluid secretion? While the inhibition of HCO_3^- secretion may be unexpected, it may serve to enhance fluid secretion into the intestinal lumen in vivo. The majority of HCO_3^- secretion and NaCl absorption takes place in the anterior intestine, leading to a hypertonic absorbate of 650 mosmol/kg H_2O within the lateral interspace (*lis*) that drives fluid absorption (23, 28). Under normal conditions, intestinal tissues can produce luminal HCO_3^- concentrations as high as 100 mmol/l, and precipitation of HCO_3^- by Ca^{2+} (and to a lesser extent Mg^{2+}) can lead to luminal osmolalities being reduced by 70–100 mosmol/kg H_2O (47, 64–66). Furthermore, luminal titration of HCO_3^- by H^+ secretion across the apical membrane by VHA further decreases the osmolality of the intestinal lumen by 20–30 mosmol/kg H_2O (25). Both these processes rely on luminal HCO_3^- and promote water absorption (47). The present study reveals that eel RGN inhibits HCO_3^- secretion, which, *in vivo*, would act to elevate luminal osmolality due to reduced precipitate formation and limited HCO_3^- titration. Thus, by inhibiting HCO_3^- secretion in the posterior intestine, the increased osmotic pressure generated by unbound Ca^{2+} and Mg^{2+}, untitrated H^+, and secreted Cl^- (due to apical CFTR activation) would draw fluid from the blood.

Conclusion. In both the Gulf toadfish and Japanese eel, guanylin peptide stimulation leads to a reversal of the absorptive I_{sc} of the posterior intestine, but not the anterior intestine. In contrast, the entire length of the mammalian intestine responds to the GN and UGN. The present study clearly demonstrates that guanylin peptide stimulation in the Gulf toadfish drives net Cl^- and fluid secretion in the posterior intestine, but, in contrast to mammals, results in the inhibition of HCO_3^- secretion. The present study demonstrates inhibited HCO_3^- secretion during CFTR-stimulated Cl^- secretion and also reveals a lack of inhibition of HCO_3^- secretion following mucosal application of CFTRinh-172. These results indicate that apical CFTR is not permeable to HCO_3^-, at least in the Gulf toadfish intestine. Additionally, the present study also provides immunohistological evidence for a potential Cl^--secretory pathway via apical CFTR and basolateral NKCC1, present only in the posterior intestine, which could drive the observed Cl^- and fluid secretion. Nevertheless, the contribution of the seemingly counterproductive fluid secretion by the distal intestine in osmoregulation remains to be investigated.

Perspectives and Significance

The traditional view of the marine teleost intestine is that of a net absorbing epithelium, for the purposes of rehydration. However, the present and previous studies (68) demonstrate a robust secretory response in the distal intestinal segments following application of guanylin peptides. Furthermore, it is demonstrated that multiple plasma membrane transporters, such as SLC26a6 and NBCe1 (a basolateral Na^+/HCO_3^--contransporter), in addition to apical CFTR or NKCC1, may be acted on by the guanylin peptides, based on the observed inhibition of HCO_3^- secretion. Indeed, a recent study revealed that UGN injected into mice resulted in decreased mRNA and protein expression of renal pendrin/SLC26a4, another Na^+/HCO_3^- cotransporter (51). Future studies should examine if the guanylin peptides affect the activity of SLC26a6 and NBCe1.

The secretory response of the distal intestinal segments to the guanylin peptides may play a role in SW osmoregulation, as suggested by stimulated peptide gene expression in eels, following their transfer from FW to SW (10–12, 39, 67, 69). While the secretory response seems counterintuitive to the normal osmoregulatory function of the marine teleost intestine, it might facilitate the elimination of solid objects remaining after digestion and/or $CaCO_3$ precipitates that are formed in the marine teleost intestine. Clearly, the integrative function of the guanylin peptides in marine teleosts demands further study. Such studies should investigate the effect of salinity and other environmental factors on GN and UGN peptide expression and release into the intestinal lumen (where they act in an auto- and paracrine fashion) to shed light on the overall whole animal function of these potent peptides.

ACKNOWLEDGMENTS

We thank Drs. M. Danielle McDonald, Douglas L. Crawford, Marjorie F. Oleksiak, and Michael C. Schmale from the Rosenstiel School of Marine and Atmospheric Science at the University of Miami for the generous use of their equipment.

Present addresses: C. Bodinier, HSE Division, Sanofi-Aventis Paris, France; A. J. Esbaugh, Marine Science Institute, University of Texas at Austin, Port Aransas, TX.

GRANTS

M. Grosell is Maytag Professor of Ichthyology and is supported by National Science Foundation Grant IOS 1146695.

DISCLOSURES

No conflicts of interest, financial or otherwise, are declared by the author(s).

AUTHOR CONTRIBUTIONS

Author contributions: I.M.R. and M.G. conception and design of research; I.M.R., C.B., E.M.M., A.J.E., C.W., and M.G. performed experiments; I.M.R. and M.G. analyzed data; I.M.R., Y.T., and M.G. interpreted results of experiments; I.M.R. and C.B. prepared figures; I.M.R. drafted manuscript; I.M.R., Y.T., and M.G. edited and revised manuscript; M.G. approved final version of manuscript.

REFERENCES

1. **Akiba Y, Jung M, Ouk S, Kaunitz JD.** A novel small molecule CFTR inhibitor attenuates HCO_3^- secretion and duodenal ulcer formation in rats. *Am J Physiol Gastrointest Liver Physiol* 289: G753–G759, 2005.
2. **Allen A, Flemström G.** Gastroduodenal mucus bicarbonate barrier: protection against acid and pepsin. *Am J Physiol Cell Physiol* 288: C1–C19, 2005.
3. **Arshad N, Visweswariah SS.** Cyclic nucleotide signaling in intestinal epithelia: getting to the gut of the matter. *Wiley Interdisciplinary Reviews: Systems Biology and Medicine*. Hoboken, NJ: Wiley, 2013.
4. **Arshad N, Visweswariah SS.** The multiple and enigmatic roles of guanylyl cyclase C in intestinal homeostasis. *FEBS Lett* 586: 2835–2840, 2012.
5. **Bengtsson MW, Jedstedt G, Flemström G.** Duodenal bicarbonate secretion in rats: stimulation by inta-arterial and luminal guanylin and uroguanylin. *Acta Physiol (Oxf)* 191: 309–317, 2007.
6. **Bodinier C, Boulo V, Lorin-Nebel C, Charmantier G.** Influence of salinity on the localization and expression of the CFTR chloride channel in the ionocytes of Dicentrarchus labrax during ontogeny. *J Anat* 214: 318–329, 2009.
7. **Bodinier C, Lorin-Nebel C, Charmantier G, Boulo V.** Influence of salinity on the localization and expression of the CFTR chloride channel in the ionocytes of juvenile Dicentrarchus labrax exposed to seawater and freshwater. *Comp Biochem Physiol A Mol Integr Physiol* 153: 345–351, 2009.

8. **Carrithers S, Jackson B, Cai W, Greenberg R, Ott C.** Site-specific effects of dietary salt intake on guanylin and uroguanylin mRNA expression in rat intestine. *Regul Pept* 107: 87–95, 2002.
9. **Chao AC, de Sauvage FJ, Dong Y, Wagner J, Goeddel D, Gardner P.** Activation of intestinal CFTR Cl^- channel by heat-stable enterotoxin and guanylin via cAMP-dependent protein kinase. *EMBO J* 13: 1065, 1994.
10. **Comrie MM, Cutler CP, Cramb G.** Cloning and expression of guanylin from the European eel (*Anguilla anguilla*). *Biochem Biophys Res Commun* 281: 1078–1085, 2001.
11. **Comrie MM, Cutler CP, Cramb G.** Cloning and expression of two isoforms of guanylate cyclase C (GC-C) from the European eel (*Anguilla anguilla*). *Comp Biochem Physiol B Biochem Mol Biol* 129: 575–586, 2001.
12. **Cramb G, Martinez AS, McWilliam I, Wilson GD.** Cloning and expression of guanylin-like peptides in teleost fish. *Ann NY Acad Sci* 1040: 277–280, 2005.
13. **Currie MG, Fok KF, Kato J, Moore RJ, Hamra FK, Duffin KL, Smith CE.** Guanylin: an endogenous activator of intestinal guanylate cyclase. *Proc Natl Acad Sci USA* 89: 947–951, 1992.
14. **Cutler CP, Cramb G.** Two isoforms of the $Na^+/K^+/2Cl^-$ cotransporter are expressed in the European eel (*Anguilla anguilla*). *Biochim Biophys Acta* 1566: 92–103, 2002.
15. **De Sauvage FJ, Keshav S, Kuang WJ, Gillett N, Henzel W, Goeddel DV.** Precursor structure, expression, and tissue distribution of human guanylin. *Proc Natl Acad Sci USA* 89: 9089–9093, 1992.
16. **Diaz M, Lorenzo A, Badia P, Gomez T.** The role of aldosterone in water and electrolyte transport across the colonic epithelium of the lizard, *Gallotia galloti*. *Comp Biochem Physiol A Comp Physiol* 91: 71–77, 1988.
17. **Forte LR.** Guanylin regulatory peptides: structures, biological activities mediated by cyclic GMP and pathobiology. *Regul Pept* 81: 25–39, 1999.
18. **Frizzell RA, Smith PL, Vosburgh E, Field M.** Coupled sodium-chloride influx across brush border of flounder intestine. *J Membr Biol* 46: 27–39, 1979.
19. **Genz J, Grosell M.** *Fundulus heteroclitus* acutely transferred from seawater to high salinity require few adjustments to intestinal transport associated with osmoregulation. *Comp Biochem Physiol A Comp Physiol* 160: 156–165, 2011.
20. **Gregório SF, Carvalho ES, Encarnação S, Wilson JM, Power DM, Canário AV, Fuentes J.** Adaptation to different salinities exposes functional specialization in the intestine of the sea bream (*Sparus aurata L.*). *J Exp Biol* 216: 470–479, 2013.
21. **Grosell M.** Intestinal anion exchange in marine fish osmoregulation. *J Exp Biol* 209: 2813–2827, 2006.
22. **Grosell M.** Intestinal anion exchange in marine teleosts is involved in osmoregulation and contributes to the oceanic inorganic carbon cycle. *Acta Physiol (Oxf)* 202: 421–434, 2011.
23. **Grosell M.** The role of the gastrointestinal tract in salt and water balance. In: *Fish Physiology*. New York: Academic, 2010, p. 135–164.
24. **Grosell M, Genz J.** Ouabain-sensitive bicarbonate secretion and acid absorption by the marine teleost fish intestine play a role in osmoregulation. *Am J Physiol Regul Integr Comp Physiol* 291: R1145–R1156, 2006.
25. **Grosell M, Genz J, Taylor J, Perry S, Gilmour K.** The involvement of H^+-ATPase and carbonic anhydrase in intestinal HCO_3^- secretion in seawater-acclimated rainbow trout. *J Exp Biol* 212: 1940–1948, 2009.
26. **Grosell M, Laliberte C, Wood S, Jensen FB, Wood C.** Intestinal HCO_3^- secretion in marine teleost fish: evidence for an apical rather than a basolateral Cl^-/HCO_3^- exchanger. *Fish Physiol Biochem* 24: 81–95, 2001.
27. **Grosell M, Mager E, Williams C, Taylor J.** High rates of HCO_3^- secretion and Cl^- absorption against adverse gradients in the marine teleost intestine: the involvement of an electrogenic anion exchanger and H^+-pump metabolon? *J Exp Biol* 212: 1684–1696, 2009.
28. **Grosell M, Taylor JR.** Intestinal anion exchange in teleost water balance. *Comp Biochem Physiol A Comp Physiol* 148: 14–22, 2007.
29. **Grosell M, Wood C, Wilson R, Bury N, Hogstrand C, Rankin C, Jensen FB.** Bicarbonate secretion plays a role in chloride and water absorption of the European flounder intestine. *Am J Physiol Regul Integr Comp Physiol* 288: R936–R946, 2005.
30. **Guba M, Kuhn M, Forssmann W, Classen M, Gregor M, Seidler U.** Guanylin strongly stimulates rat duodenal HCO_3^- secretion: proposed mechanism and comparison with other secretagogues. *Gastroenterology* 111: 1558–1568, 1996.
31. **Guffey S, Esbaugh A, Grosell M.** Regulation of apical H^+-ATPase activity and intestinal HCO_3^- secretion in marine fish osmoregulation. *Am J Physiol Regul Integr Comp Physiol* 301: R1682–R1691, 2011.
32. **Hallbäck D, Jodal M, Mannischeff M, Lundgren O.** Tissue osmolality in intestinal villi of four mammals in vivo and in vitro. *Acta Physiol Scand* 143: 271–277, 1991.
33. **Halm D, Krasny E, Frizzell R.** Electrophysiology of flounder intestinal mucosa. II. Relation of the electrical potential profile to coupled NaCl absorption. *J Gen Physiol* 85: 865–883, 1985b.
34. **Hamra FK, Eber SL, Chin DT, Currie MG, Forte LR.** Regulation of intestinal uroguanylin/guanylin receptor-mediated responses by mucosal acidity. *Proc Natl Acad Sci USA* 94: 2705–2710, 1997.
35. **Hiroi J, Yasumasu S, McCormick SD, Hwang PP, Kaneko T.** Evidence for an apical Na-Cl cotransporter involved in ion uptake in a teleost fish. *J Exp Biol* 211: 2584–2599, 2008.
36. **Iio K, Nakauchi M, Yamagami S, Tsutsumi M, Hori H, Naruse K, Mitani H, Shima A, Suzuki N.** A novel membrane guanylyl cyclase expressed in medaka (*Oryzias latipes*) intestine. *Comp Biochem Physiol B Biochem Mol Biol* 140: 569–578, 2005.
37. **Ishiguro H, Steward MC, Naruse S, Ko SB, Goto H, Case RM, Kondo T, Yamamoto A.** CFTR functions as a bicarbonate channel in pancreatic duct cells. *J Gen Physiol* 133: 315–326, 2009.
38. **Joo NS, London RM, Kim HD, Forte LR, Clarke LL.** Regulation of intestinal Cl^- and secretion by uroguanylin. *Am J Physiol Gastrointest Liver Physiol* 274: G633–G644, 1998.
39. **Kalujnaia S, Wilson GD, Feilen AL, Cramb G.** Guanylin-like peptides, guanylate cyclase and osmoregulation in the European eel (*Anguilla anguilla*). *Gen Comp Endocrinol* 161: 103–114, 2009.
40. **Kita T, Kitamura K, Sakata J, Eto T.** Marked increase of guanylin secretion in response to salt loading in the rat small intestine. *Am J Physiol Gastrointest Liver Physiol* 277: G960–G966, 1999.
41. **Kopeikin Z, Sohma Y, Li M, Hwang TC.** On the mechanism of CFTR inhibition by a thiazolidinone derivative. *J Gen Physiol* 136: 659–671, 2010.
42. **Kuhn M, Adermann K, Jähne J, Forssmann W, Rechkemmer G.** Segmental differences in the effects of guanylin and *Escherichia coli* heat-stable enterotoxin on Cl^- secretion in human gut. *J Physiol* 479: 433–440, 1994.
43. **Kurita Y, Nakada T, Kato A, Doi H, Mistry AC, Chang MH, Romero MF, Hirose S.** Identification of intestinal bicarbonate transporters involved in formation of carbonate precipitates to stimulate water absorption in marine teleost fish. *Am J Physiol Regul Integr Comp Physiol* 294: R1402–R1412, 2008.
44. **Kusakabe T, Suzuki N.** The guanylyl cyclase family in medaka fish *Oryzias latipes*. *Zoolog Sci* 17: 131–140, 2000.
45. **Li Z, Knowles JW, Goyeau D, Prabhakar S, Short DB, Perkins AG, Goy MF.** Low salt intake down-regulates the guanylin signaling pathway in rat distal colon. *Gastroenterology* 111: 1714–1721, 1996.
46. **Li Z, Lui EY, Wilson JM, Ip YK, Lin Q, Lam TJ, Lam SH.** Expression of key ion transporters in the gill and esophageal-gastrointestinal tract of euryhaline Mozambique tilapia Oreochromis mossambicus acclimated to fresh water, seawater and hypersaline water. *PLoS One* 9: e87591, 2014.
47. **Marshall W, Grosell M.** Ion transport, osmoregulation, and acid-base balance. *Physiol Fish* 3: 177–230, 2006.
48. **Marshall W, Howard J, Cozzi R, Lynch E.** NaCl and fluid secretion by the intestine of the teleost *Fundulus heteroclitus*: involvement of CFTR. *J Exp Biol* 205: 745–758, 2002.
49. **McDonald MD, Grosell M, Wood CM, Walsh PJ.** Branchial and renal handling of urea in the Gulf toadfish, *Opsanus beta*: the effect of exogenous urea loading. *Comp Biochem Physiol A Comp Physiol* 134: 763–776, 2003.
50. **Müller T, Dieplinger B.** The guanylin peptide family and the proposed gastrointestinal-renal natriuretic signaling axis. *Kidney Int* 82: 1253–1255, 2012.
51. **Rozenfeld J, Tal O, Kladnitsky O, Adler L, Efrati E, Carrithers SL, Alper SL, Zelikovic I.** The pendrin anion exchanger gene is transcriptionally regulated by uroguanylin: a novel enterorenal link. *Am J Physiol Renal Physiol* 302: F614–F624, 2012.
52. **Schulz S, Chrisman T, Garbers D.** Cloning and expression of guanylin. Its existence in various mammalian tissues. *J Biol Chem* 267: 16019–16021, 1992.
53. **Schulz S, Green CK, Yuen PS, Garbers DL.** Guanylyl cyclase is a heat-stable enterotoxin receptor. *Cell* 63: 941–948, 1990.
54. **Seidler U, Blumenstein I, Kretz A, Viellard-Baron D, Rossmann H, Colledge W, Evans M, Ratcliff R, Gregor M.** A functional CFTR protein is required for mouse intestinal cAMP-, cGMP- and Ca^2-dependent HCO_3^- secretion. *J Physiol* 505: 411–423, 1997.

55. **Singer TD, Tucker SJ, Marshall WS, Higgins CF.** A divergent CFTR homologue: highly regulated salt transport in the euryhaline teleost *F. heteroclitus. Am J Physiol Cell Physiol* 274: C715–C723, 1998.
56. **Smith HW.** The absorption and excretion of water and salts by marine teleosts. *Am J Physiol* 93: 480–505, 1930.
57. **Spiegel S, Phillipper M, Rossmann H, Riederer B, Gregor M, Seidler U.** Independence of apical Cl^-/HCO_3^- exchange and anion conductance in duodenal HCO_3^- secretion. *Am J Physiol Gastrointest Liver Physiol* 285: G887–G897, 2003.
58. **Takei Y, Kawakoshi A, Tsukada T, Yuge S, Ogoshi M, Inoue K, Hyodo S, Bannai H, Miyano S.** Contribution of comparative fish studies to general endocrinology: structure and function of some osmoregulatory hormones. *J Exp Zool A Comp Exp Biol* 305: 787–798, 2006.
59. **Takei Y, Yuge S.** The intestinal guanylin system and seawater adaptation in eels. *Gen Comp Endocrinol* 152: 339–351, 2007.
60. **Taylor J, Mager E, Grosell M.** Basolateral NBCe1 plays a rate-limiting role in transepithelial intestinal HCO_3^- secretion, contributing to marine fish osmoregulation. *J Exp Biol* 213: 459–468, 2010.
61. **Toriano R, Ozu M, Politi MT, Dorr RA, Curto MA, Capurro C.** Uroguanylin regulates net fluid secretion via the NHE2 isoform of the Na^+/H^+ exchanger in an intestinal cellular model. *Cell Physiol Biochem* 28: 733–742, 2011.
62. **Tresguerres M, Levin LR, Buck J, Grosell M.** Modulation of NaCl absorption by $[HCO_3^-]$ in the marine teleost intestine is mediated by soluble adenylyl cyclase. *Am J Physiol Regul Integr Comp Physiol* 299: R62–R71, 2010.
63. **Wilson R, Gilmour K, Henry R, Wood C.** Intestinal base excretion in the seawater-adapted rainbow trout: a role in acid-base balance? *J Exp Biol* 199: 2331–2343, 1996.
64. **Wilson R, Millero F, Taylor J, Walsh P, Christensen V, Jennings S, Grosell M.** Contribution of fish to the marine inorganic carbon cycle. *Science* 323: 359–362, 2009.
65. **Wilson RW, Grosell M.** Intestinal bicarbonate secretion in marine teleost fish - source of bicarbonate, pH sensitivity, and consequences for whole animal acid-base and calcium homeostasis. *Biochim Biophys Acta* 1618: 163–174, 2003.
66. **Wilson RW, Wilson JM, Grosell M.** Intestinal bicarbonate secretion by marine teleost fish–why and how? *Biochim Biophys Acta* 1566: 182–193, 2002.
67. **Yuge S, Inoue K, Hyodo S, Takei Y.** A novel guanylin family (guanylin, uroguanylin, and renoguanylin) in eels: possible osmoregulatory hormones in intestine and kidney. *J Biol Chem* 278: 22726–22733, 2003.
68. **Yuge S, Takei Y.** Regulation of ion transport in eel intestine by the homologous guanylin family of peptides. *Zoolog Sci* 24: 1222–1230, 2007.
69. **Yuge S, Yamagami S, Inoue K, Suzuki N, Takei Y.** Identification of two functional guanylin receptors in eel: Multiple hormone-receptor system for osmoregulation in fish intestine and kidney. *Gen Comp Endocrinol* 149: 10–20, 2006.